

UC Irvine

UC Irvine Previously Published Works

Title

Enhanced Cellular Responses and Distinct Gene Profiles in Human Fetoplacental Artery Endothelial Cells under Chronic Low Oxygen¹

Permalink

<https://escholarship.org/uc/item/2r54q62f>

Journal

Biology of Reproduction, 89(6)

ISSN

0006-3363

Authors

Jiang, Yi-Zhou
Wang, Kai
Li, Yan
[et al.](#)

Publication Date

2013-12-01

DOI

10.1095/biolreprod.113.110551

Peer reviewed

Enhanced Cellular Responses and Distinct Gene Profiles in Human Fetoplacental Artery Endothelial Cells under Chronic Low Oxygen¹

Yi-Zhou Jiang,⁴ Kai Wang,^{4,5} Yan Li,⁴ Cai-Feng Dai,^{3,4} Ping Wang,⁶ Christina Kendzierski,⁶ Dong-Bao Chen,⁷ and Jing Zheng^{2,4}

⁴Department of Obstetrics and Gynecology, University of Wisconsin, Madison, Wisconsin

⁵Clinical and Translational Research Center, Shanghai First Maternity and Infant Hospital, Tongji University School of Medicine, Shanghai, China

⁶Department of Biostatistics and Medical Informatics, University of Wisconsin, Madison, Wisconsin

⁷Department of Obstetrics and Gynecology, University of California, Irvine, California

ABSTRACT

Fetoplacental endothelial cells are exposed to oxygen levels ranging from 2% to 8% *in vivo*. However, little is known regarding endothelial function within this range of oxygen because most laboratories use ambient air (21% O₂) as a standard culture condition (SCN). We asked whether human umbilical artery endothelial cells (HUAECs) that were steadily exposed to the physiological chronic normoxia (PCN, 3% O₂) for ~20–25 days differed in their proliferative and migratory responses to FGF2 and VEGFA as well as in their global gene expression compared with those in the SCN. We observed that PCN enhanced FGF2- and VEGFA-stimulated cell proliferation and migration. In oxygen reversal experiments (i.e., when PCN cells were exposed to SCN for 24 h and vice versa), we found that preexposure to 21% O₂ decreased the migratory ability, but not the proliferative ability, of the PCN-HUAECs in response to FGF2 and VEGFA. These PCN-enhanced cellular responses were associated with increased protein levels of HIF1A and NOS3, but not FGFR1, VEGFR1, and VEGFR2. Microarray analysis demonstrated that PCN up-regulated 74 genes and down-regulated 86, 14 of which were directly regulated by hypoxia-inducible factors as evaluated using *in silico* analysis. Gene function analysis further indicated that the PCN-regulated genes were highly related to cell proliferation and migration, consistent with the results from our functional assays. Given that PCN significantly alters cellular responses to FGF2 and VEGFA as well as transcription in HUAECs, it is likely that we may need to reexamine the current cellular and molecular mechanisms controlling fetoplacental endothelial functions, which were

largely derived from endothelial models established under ambient O₂.

angiogenesis, artery endothelial cells, growth factors, physiological chronic low oxygen, transcriptome

INTRODUCTION

Human pregnancy is associated with dramatic increases in fetoplacental blood flows, which are directly correlated with fetal growth and survival as well as neonatal birth weights and survivability [1, 2]. These increases in placental blood flows primarily result from angiogenesis, vasodilation, and vascular remodeling, and vascular endothelial cells play a central role in all of these processes [3–5]. Placental endothelial cells live in lower O₂ environments (~2%–8% O₂ or 15–60 mmHg pO₂, ~2% O₂ at ≤8–10 wk of gestation, ~8% O₂ between 8 to 10 wk, and ~6% O₂ at the end of the third trimester) relative to ambient O₂ (~21% or 160 mmHg pO₂ at sea level) or mean arterial O₂ (~13% or 100 mmHg pO₂ at sea level) [6]. These physiological chronic low O₂ levels are believed to be critical for maintaining normal vascular growth and function to support the growing placenta and fetus [7–9]. In contrast, many diseases associated with endothelial dysfunction such as preeclampsia and atherosclerosis-induced chronic ischemia are often accompanied by an even lower pO₂ [10–13]. Our current understanding on cellular and molecular mechanisms controlling human fetoplacental endothelial functions, however, is largely derived from umbilical vein endothelial cell models, most of which were established under ambient O₂. This ambient O₂ level obviously does not closely mimic the environment in which these cells reside *in vivo* [6]. Thus, establishing fetoplacental endothelial cell models, particularly from artery cells, under the physiological chronic low O₂ is of great significance for investigating cellular and molecular mechanisms because information derived from these artery cell models will improve our understanding of fetoplacental endothelial function in physiopathological states.

In addition to O₂, various growth factors such as fibroblast growth factor 2 (FGF2) and vascular endothelial growth factor A (VEGFA) also closely mediate endothelial function via activation of their high affinity receptors and downstream signaling cascades [5, 14–16]. Numerous studies have demonstrated that exposing endothelial cells established under ambient O₂ to low O₂ levels (~2%–5% O₂; 4–120 h) promotes endothelial proliferation and migration [17–20], primarily through elevating the expression of growth factors and their receptors such as VEGFA and VEGFA receptor 2 (VEGFR2) [10, 11].

¹Supported in part by National Institutes of Health grants PO1 HD38843 to R.R. Magness and J.Z.; a Department of Ob/Gyn R & D Grant, University of Wisconsin-Madison, to J.Z.; R01 HL74947& HL70562 to D.B.C.; and the National Science Foundation of China No. 81100429 and Shanghai Natural Science Foundation No.11 ZR1428700 to K.W. The microarray data were logged in Gene Expression Omnibus at National Center for Biotechnology Information (GEO access no. GSE49958 at www.ncbi.nlm.nih.gov/geo).

²Correspondence: Jing Zheng, Department of Obstetrics and Gynecology, University of Wisconsin, PAB1 Meriter Hospital, 202 S. Park St., Madison, WI 53715. E-mail: jzheng@wisc.edu

³Current addresses: Center for Reproductive Medicine, Qilu Hospital of Shandong University, Jinan 250012, China.

Received: 7 May 2013.

First decision: 25 June 2013.

Accepted: 15 October 2013.

© 2013 by the Society for the Study of Reproduction, Inc.

eISSN: 1529-7268 <http://www.biolreprod.org>

ISSN: 0006-3363

Recently, we have reported that in human umbilical vein endothelial cells (HUVECs), physiological chronic normoxia (3% O₂ for 20–25 days) robustly alters transcriptional profiles and cellular responses compared with those in ambient O₂ [21]. However, little is known regarding the physiological normoxia (2%–13% O₂) [10, 11] regulation of transcription and the subsequent response to FGF2 and VEGFA in human fetoplacental artery endothelial cells. The investigation of fetoplacental artery endothelial cells is of particular significance because endothelial cells with different origins are extremely heterogeneous in their transcriptional profiles [22], which may lead to distinct cellular morphologies and responses to the same stimuli (e.g., low O₂ and growth factors) [5, 23, 24]. For example, placental growth factors-1 and -2 (PlGF-1 and PlGF-2) effectively stimulated cell proliferation in human placental microvascular endothelial cells, but not in HUVECs, while VEGFA and FGF2 similarly induce the proliferation of human placental microvascular endothelial cells and HUVECs [25]. In addition, it has also been shown that hypoxia (1% O₂, 24 h) enhances expression and activity of endothelial nitric oxide synthase (NOS3) in aortic endothelial cells [26], whereas hypoxia decreases the total NOS3 protein levels and activity in coronary artery endothelial cells [27]. Thus, assessing cell responses to low O₂ and growth factors in endothelial cells of different origins is critical for our better understanding of endothelial and vascular physiology.

Compared with their counterparts HUVECs, human umbilical artery endothelial cells (HUAECs) *in vivo* are also constantly exposed to O₂ that are lower than the ambient O₂ level during pregnancy. At term, the O₂ level is ~2.0% (range: 1.1%–2.9%) in the umbilical cord artery, which is lower than the ~3.5% O₂ (range: 2.4%–4.6%) in the umbilical cord vein [28]. To explore the role of physiological chronic low O₂ in HUAECs, in this study, we examined the cell proliferation and migration in responses to FGF2 and VEGFA in HUAECs that were expanded continuously under standard cell culture normoxia (21% O₂) or under physiological chronic normoxia (3% O₂ for ~20–25 days). We also examined and compared the transcriptional profiles of these HUAECs using microarray analysis.

MATERIALS AND METHODS

An additional methods section is available in the Supplemental Materials and Methods (all the Supplemental Data are available online at www.biolreprod.org).

Reagent and Chemicals

Unless stated otherwise, the reagents and chemicals were purchased from Sigma-Aldrich.

Endothelial Cultures

Human umbilical cords from normal term pregnant patients with no medical complications were collected immediately (≤ 1 h) after Cesarean section as previously described [21]. The cord collection protocol was approved by the Institutional Review Board of Meriter Hospital and the Health Sciences Institutional Review Boards, University of Wisconsin-Madison. HUAECs were isolated using a standard collagenase enzyme digestion, expanded, and characterized as previously described [20, 21]. Immediately after isolation, cells obtained from the same artery were split equally, cultured, and expanded steadily under standard cell culture normoxia (37°C, 5% CO₂, 95% air; designated as SCN) or physiological chronic normoxia (37°C, 5% CO₂, 3% O₂, 92% N₂; designated as PCN) for up to 25 days. The cells were cultured in RPMI 1640 medium (Invitrogen) supplemented with 10% fetal bovine serum (HyClone), 1% penicillin/streptomycin (HyClone), 100 mg/L heparin (EMD Millipore), and 37.5 mg/L endothelial cell growth supplement (Millipore). For the PCN culture and treatments, the media were prepurged with N₂ and equilibrated in a hypoxia incubator before being added to the cells. The

dissolved O₂ in the media was monitored using a dissolved oxygen meter (Mettler Toledo). PCN was also confirmed by determining the cellular protein levels as following: hypoxia inducible factor 1, alpha subunit (HIF1A); BCL2/adenovirus E1B 19 kDa interacting protein 3 (BNIP3); and solute carrier family 2 (facilitated glucose transporter), member 3 (SLC2A3; also termed glucose transporter 3, i.e., GLUT3).

After 3–4 days of culture, the cells were sorted by flow cytometry based on their expression of platelet/endothelial cell adhesion molecule 1 (PECAM 1, also known as CD31). The cell purity was also examined by uptake of 10 μ g/ml 1,1'-dioctadecyl-3,3,3',3'-tetramethyl-indocarbocyanine perchlorate (DiI-Ac-LDL; Biomedical Technologies). At passage one, the cells were subjected to the capillarylike tube formation assay to further confirm their endothelial phenotype. Only the cell preparations in which $\geq 96\%$ of the cells were positive for CD31, exhibited DiI-Ac-LDL uptake, and were capable of forming capillarylike tube structures were utilized in this study. The cells at passage three (~15 days after isolation) were used for the microarray study, while cells at passages four to five (~20–25 days after isolation) were used for all the other studies.

Paired SCN and PCN HUAECs, derived from the same artery were used for all the conducted experiments. All the 3% O₂ experiments were performed in a heated oxygen-controlled glove box (Coy Laboratory Products), and the media were prepurged with N₂ and equilibrated to 3% O₂ before being added to the cells.

Cell Surface Area and Diameter Measurements

The cell surface area and diameter were determined as previously described [21]. Briefly, cells (100,000 cells/well) were seeded in a six-well plate and cultured for 16 h to allow cell attachment. To measure the cell surface area, attached cells at a nonconfluent state were incubated with 1 μ M 5-chloromethylfluorescein diacetate (Cell Tracker Green; Invitrogen) at 37°C for 45 min. After washing, the cells were examined under a microscope and cell images were recorded. The cell surface area of each individual cell was analyzed using MetaMorph software (Molecular Devices). To measure the diameter of viable cells, the attached cells were lifted up by trypsin digestion, resuspended in PBS, and stained with trypan blue. The mean cell diameter was determined using an automated cell counter (Countess; Invitrogen).

Cell Proliferation and Migration Assays

A cell proliferation assay was performed using a bromodeoxyuridine (BrdU) kit (EMD Millipore) as previously described [21, 29]. The cells seeded in 96-well plates (8000 cells/well) were cultured for 16 h. After 8 h of serum starvation, the cells were treated with 0, 1, 10, or 100 ng/ml of FGF2 or VEGFA for 16 h, labeled with BrdU for 8 h, and then fixed and probed with anti-BrdU antibody. The signals were detected using a microplate reader (Synergy HT Multi-Mode; BioTek). Cell migration was evaluated using a 24-multiwell FluoroBlok transwell insert system (BD Biosciences) [21, 30]. After 8 h of serum starvation, cells were seeded into inserts, followed by adding 0, 10, or 100 ng/ml of FGF2 or VEGFA in the bottom wells. After 16 h of incubation, calcein acetoxymethyl ester, a fluorescent dye (final concentration 0.5 μ g/ml; Invitrogen) was added to the bottom wells and incubated for 30 min. Migrated cells were recorded (four randomly chosen fields/well, average 52 cells/field in the control) under a Nikon inverted microscope (10 \times objective) connected to a charge-coupled device camera. The cell numbers were counted using Metamorph image analysis software (Molecular Devices). These doses of FGF2 and VEGFA were chosen based on our previous studies on human placental artery endothelial cells [20] and HUVECs [21]. These doses of FGF2 or VEGFA also appear to fall within the range of their physiological concentrations, although the reports on the physiological concentrations of FGF2 and VEGFA in the umbilical artery are limited. For example, Hill et al. [31] have reported that the FGF2 concentration in cord blood at term is ~2 ng/ml as measured by radioimmunoassay [32], while VEGFA concentration is ~10 ng/ml [31] or 1.4 ng/ml using the enzyme-linked immunosorbent assay [33]. However, other investigators have observed much low levels of unbound FGF2 (39.75 \pm 19.87 pg/ml) and VEGFA (422.83 \pm 386.10 pg/ml) in the umbilical artery serum at term as measured using the enzyme-linked immunosorbent assay kit [34]. Thus, the FGF2 and VEGFA levels in the cord blood might be highly variable, possibly depending on the measurement method [35]. To determine the sustainability/reversibility of the SCN- or PCN-programmed cell proliferation and migration, the SCN and PCN cells were cultured under 21% and 3% O₂ until reaching confluence and were then switched to 3% and 21% O₂ (note: the O₂ levels were reversed), respectively, for 1 day, followed by treatments with 10 ng/ml FGF2 and VEGFA and the BrdU and migration assays. All the 3% O₂ experiments were conducted in the hypoxic chamber with media pre-equilibrated to 3% O₂.

Microarray Analysis

Microarray hybridization and data analysis were conducted as previously described [21]. Total RNA was extracted from six pairs of cell preparations of SCN and PCN HUAECs (total 12) at 80% confluence using an RNeasy Mini Kit (Qiagen) in conjunction with a Qiagen shredder following the manufacturer's instructions [21, 36]. The total RNA was quantified using a Nanodrop ND-100 spectrophotometer (Nanodrop Technologies). The microarray facility at the University of Wisconsin Biotech Center confirmed the quality and integrity of the RNA using an Agilent RNA6000 NanoChip in the Agilent 2100 Bioanalyzer (Agilent Technologies). Only high-quality RNA samples with an integrity number ~ 9.9 (for a range 1–10, 10 is completely intact RNA) were subjected to further microarray analysis. Complementary RNA was synthesized, labeled, and fragmented using the MessageAmp II-biotin enhanced kit (Ambion). Fragmented cRNA (10 $\mu\text{g}/\text{sample}$) was hybridized to Affymetrix U133 plus 2.0 microarray chips (Affymetrix). The chips were processed on Affymetrix GC450 Fluidics station. Data were extracted from GC3000 G7 scanned images using Affymetrix Expression Console software version 1.4. Microarray hybridization and postprocessing were conducted by experienced staff at the Biotech Center. To assess the quality of the entire assay and data analysis, routine quality controls were conducted according to standard Affymetrix protocols, which include visual array inspection, 3'/5' glyceraldehyde-3-phosphate dehydrogenase (*GAPDH*) and β -actin ratios, percent present calls, B2 signal, intensity of poly-A RNA and hybridization controls, and background and noise values. A scaling factor was used to correct for variations between gene chips. The signal ratio of 3' probe sets to 5' probe sets of genes were calibrated by normalizing to the signal ratio of *GAPDH* and β -actin.

The microarray data were logged in Gene Expression Omnibus at National Center for Biotechnology Information (GEO access # GSE49958 at www.ncbi.nlm.nih.gov/geo).

Microarray Data Analyses

These data were normalized with Robust Multi-Array Analysis as previously described [21]. EBarrays [37] was applied to identify differentially expressed (DE) genes. Specifically, a gene was identified as a DE gene if its posterior probability of differential expression as assessed by EBarrays exceeded 0.99. This threshold was chosen to set the posterior expected false discovery rate to 1%. A second filter was applied to ensure that the transcripts were expressed at a detectable level. In particular, an up-regulated gene was selected only if all the probe sets in its corresponding condition were deemed present as characterized using the present/absent calls provided by Affymetrix postprocessing software (Microarray Suite Version 5.0).

Hierarchical clustering of the microarray data was performed using the MeV with Pearson correlation [38]. The DE genes were then uploaded to the Ingenuity Pathway Analysis using a manually curated relationship from the literature (www.ingenuity.com).

Quantitative PCR

Quantitative PCR (qPCR) was conducted as previously described [21]. The first strand cDNA was synthesized by SuperScript II reverse transcriptase (Invitrogen) with T7-oligo (dT) 24 primers. Quantitative PCR was performed with SYBR Green I Master (Roche) and primers (Supplemental Table S1) in a Light Cycler 480 (Roche). All the samples were run in triplicate. Negative controls (no template control and no enzyme control) were included in every set of amplification. β -Actin and TATA box binding proteins selected by BestKeeper software [39] were used for normalization. RE-ST2005 software [39, 40] was applied to determine the relative fold change. To determine whether there were statistically significant difference, RE-ST2005 calculated the probability of the alternate hypothesis that the difference between the sample and control groups was only due to chance by performing 50 000 random reallocations of the sample (PCN) and control (SCN) data.

Western Blot Analysis

Western blot analysis was performed as previously described [20, 21]. The cells were lysed by sonication in buffer (50 mM HEPES, 0.1 M NaCl, 10 mM ethylenediaminetetraacetic acid, 4 mM sodium pyrophosphate, 10 mM sodium fluoride, 2 mM sodium orthovanadate [pH 7.5], 1 mM phenylmethylsulfonyl-fluoride, 1% Triton X-100, 5 $\mu\text{g}/\text{ml}$ leupeptin, and 5 $\mu\text{g}/\text{ml}$ aprotinin). After centrifugation, the protein concentrations of the supernatant were determined with bovine serum albumin (fraction V) as the standard. The protein samples (20 μg) were separated on SDS-PAGE gels and electrically transferred to polyvinylidene fluoride membranes. The membranes were immunoblotted with

the antibody against different targets (Supplemental Table S2). The proteins were visualized using enhanced chemiluminescence reagents (Amersham Biosciences) followed by exposure to chemiluminescence films. The signals were detected using enhanced chemiluminescence or enhanced chemiluminescence-plus reagents (Amersham Biosciences) and recorded using an Epson Perfection 4990 Photo Scanner [21, 29].

Statistical Analyses for All the Studies Other than Microarray Analysis

Data were analyzed using one way analysis of variance, (SigmaStat; Jandel Co.). When an F test was significant, the data were compared with their respective control by Bonferroni multiple comparisons or Student *t*-test.

RESULTS

Characterization of HUAECs

Several approaches were taken to validate the endothelial phenotype and purity of the HUAECs. We observed that both SCN and PCN HUAECs exhibited a typical cobblestone morphology at confluence, showed uptake of DiI-Ac-LDL ($\geq 99\%$), expressed CD31 ($\geq 95\%$) (not shown), and formed capillarylike tube structures (Supplemental Fig. S1A), confirming the establishment of a highly pure population of HUAECs.

Cell Surface Area and Diameter Measurements

The mean cell surface area of an attached PCN cell ($637 \pm 35 \mu\text{m}^2$) was significantly ($P < 0.05$) smaller than that of a SCN cell ($853 \pm 57 \mu\text{m}^2$); however, the mean diameter of a single cell in suspension was similar between the SCN and PCN HUAECs (13.9 vs. 14.0 μm ; Supplemental Fig. S1, B and C). These data suggest that although the mean volumes of single PCN and SCN cells are comparable, the attached SCN cells are more spread out in the cell culture on the polystyrene surface. This finding also clearly indicates the morphological adaptations of the endothelial cells to the different O₂ levels.

Cell Proliferation and Migration

To determine the role of PCN in artery endothelial function, cell proliferation and migration assays were performed. We observed that FGF2 and VEGFA promoted ($P < 0.05$) SCN and PCN cell proliferation (Fig. 1, A and B). Importantly, PCN further enhanced ($P < 0.05$) the FGF2- and VEGFA-stimulated cell proliferation up to 2-fold (Fig. 1, A and B). To test where an acute O₂ fluctuation could affect endothelial proliferation, PCN and SCN cells were reversely cultured in 20% and 3% O₂, respectively, for 1 day. Interestingly, preexposure of SCN cells to 3% O₂ for 1 day slightly but not significantly enhanced the FGF2-stimulated cell proliferation; however this exposure significantly ($P < 0.05$) promoted the VEGFA-stimulated cell proliferation (by ~ 0.6 -fold; Fig. 1, C and D). In contrast, preexposure of PCN cells to 21% O₂ for 1 day did not alter either the FGF2- or VEGFA-stimulated cell proliferation (Fig. 1, C and D).

Both FGF2 and VEGFA also stimulated ($P < 0.05$) the SCN and PCN cell migration, while PCN further promoted ($P < 0.05$) the FGF2- (1.4- and 1.5-fold of SCN for 10 and 100 ng/ml of FGF2, respectively) and VEGFA-induced (3.3- and 2.7-fold of SCN for 10 and 100 ng/ml of VEGFA) cell migration (Fig. 2 and Supplemental Fig. S2). Preculturing SCN cells in 3% O₂ for 1 day further promoted ($P < 0.05$) the FGF2-stimulated SCN cell migration (0.6-fold) and VEGFA-stimulated SCN cell migration (0.5-fold), while preculturing PCN cells in 21% O₂ attenuated ($P < 0.05$) the FGF2-

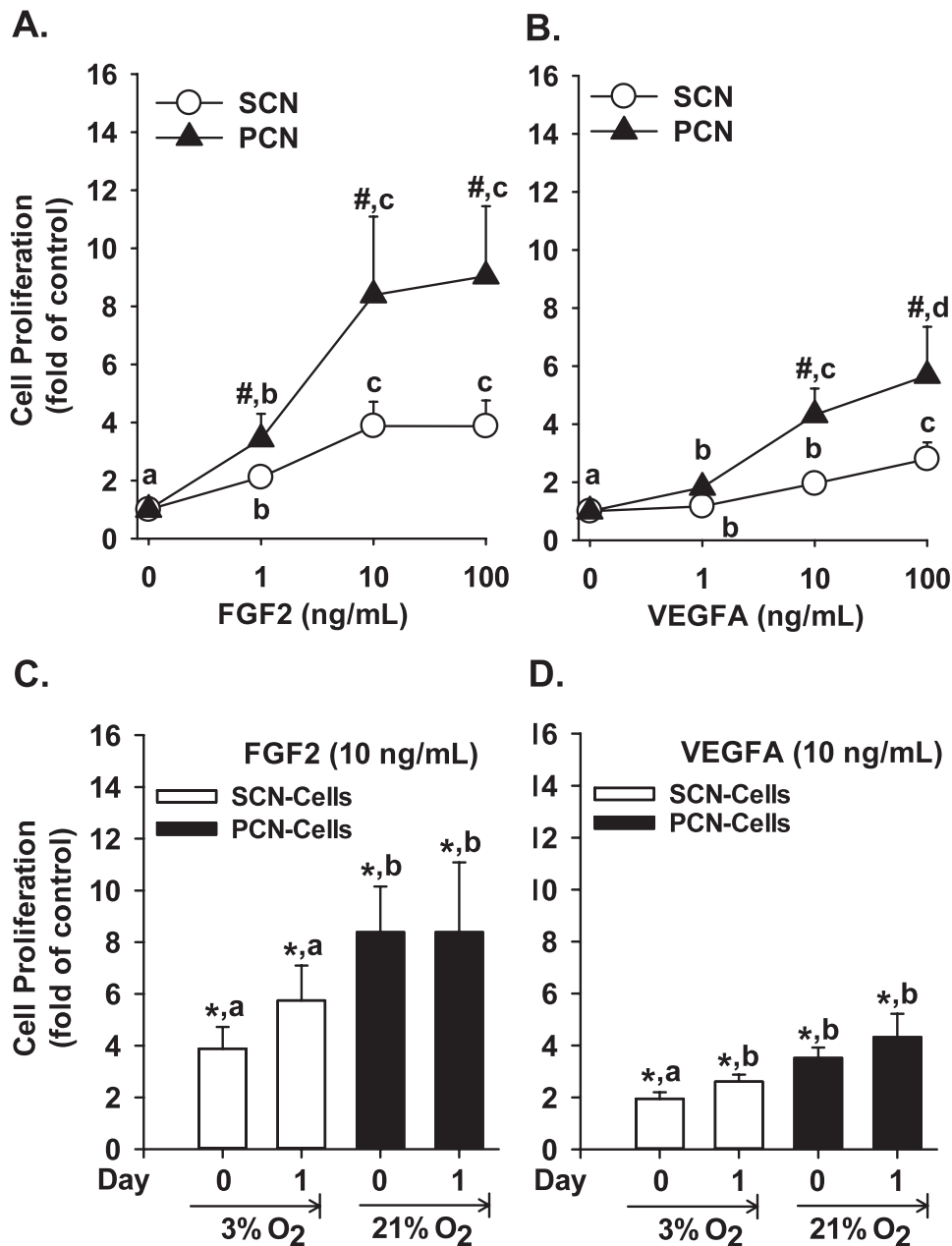


FIG. 1. FGF2- and VEGFA-stimulated SCN and PCN cell proliferation. **A, B**) SCN and PCN cells were cultured in 21% and 3% O₂, respectively. **C, D**) SCN and PCN cells were preincubated in 3% and 21% O₂, respectively, for 24 h (note: the O₂ levels were reversed). After serum starvation, cells were treated with 10 ng/ml of FGF2 and VEGFA followed by the BrdU proliferation assays. Data are expressed as the means \pm SEM fold change of the no growth factor control. #Differ from SCN at each corresponding dose ($P < 0.05$). *Differ from the corresponding no growth factor control. ^{a,b,c,d} Means with different letters differ from each other in SCN or PCN cells (**A–D**) ($P < 0.05$); $n = 6$ pairs of cell preparations.

stimulated PCN cell migration (0.8-fold) and VEGFA-stimulated PCN cell migration (1.1-fold) (Fig. 2, C and D).

These results clearly show that PCN indeed enhances cell proliferation and migration in response to FGF2 and VEGFA and that such O₂-programmed effects are relatively stable, particularly for cell proliferation. HUAECs proliferation is more sensitive to FGF2 than to VEGFA (Fig. 1), whereas HUAECs migration is more sensitive to VEGFA than to FGF2 (Fig. 2 and Supplemental Fig. S2). For example, FGF2 increased the PCN cell proliferation by ~ 8.4 -fold, whereas VEGFA did so by only ~ 3.5 -fold. Conversely, VEGFA induced a 5.5-fold increase in PCN cell migration, whereas while FGF2 caused only a 2.7-fold elevation.

Microarray Analysis

To examine whether PCN changes the global gene expression profiles of HUAECs relative to those in SCN, microarray analysis was conducted. Two-dimensional hierarchical clustering of DE genes and individual cell preparations demonstrated that the expression signatures were similar among the different cell preparations within each culture condition, but the expression signatures varied greatly between SCN and PCN HUAECs (Fig. 3A). Compared with SCN, PCN up-regulated 74 genes and down-regulated 86 (Tables 1 and Supplemental Table S3). Ingenuity pathway analysis (IPA) for these DE genes revealed a prominent enrichment of genes relevant to cellular movement, development, cellular growth

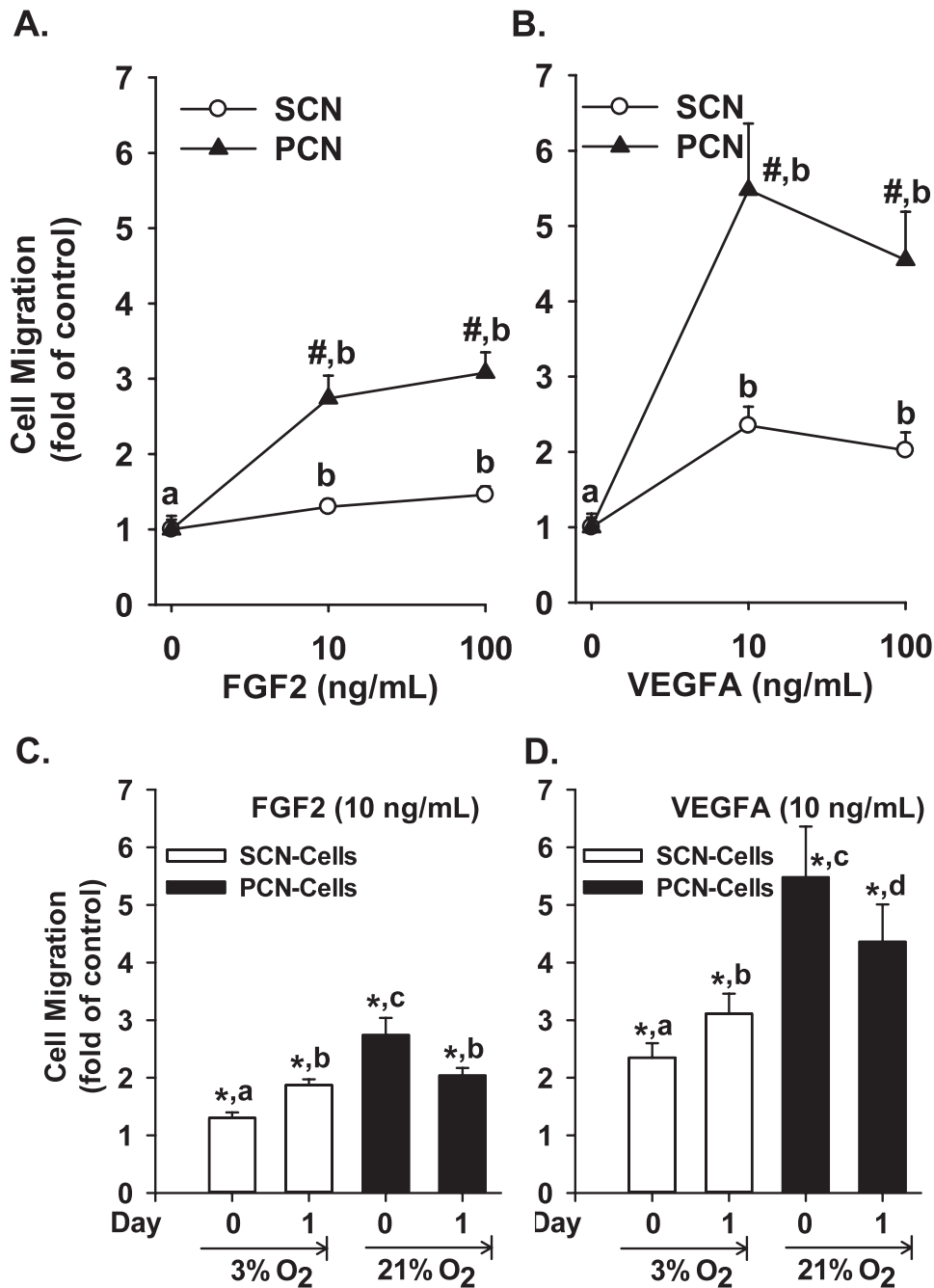


FIG. 2. FGF2- and VEGFA-stimulated SCN and PCN cell migration. **A, B**) SCN and PCN cells were cultured in 21% and 3% O₂ respectively. **C, D**) SCN and PCN cells were preincubated in 3% and 21% O₂, respectively, for 24 h (note: the O₂ levels were reversed). After serum starvation, cells were treated with FGF2 and VEGFA, followed by the migration assays. Data are expressed as the means \pm SEM fold change of the no growth factor control. *Differ from SCN at each corresponding dose ($P < 0.05$). #Differ from the corresponding no growth factor control. *a,b,c,d* Means with different letters differ from each other in SCN or PCN cells (**A–D**) ($P < 0.05$); $n = 6$ pairs of cell preparations.

and proliferation, cell death and survival, and cell morphology (Fig. 3B and Supplemental Table S4). These data indicate that PCN robustly alters global gene profiles, shifting the equilibrium in cellular function. For instance, IPA demonstrated that PCN enhanced cell viability but inhibited cellular sprouting as predicated by the positive and negative z-score, respectively (Supplemental Table S4). Literature mining by IPA further predicted that out of a total of 160 DE genes, 14 genes (8.8%) were regulated by hypoxia inducible factors (HIF) (Fig. 3C). Thus, PCN induces dramatic changes in the HUAECs transcriptional profiles compared with those in SCN,

and these changes are highly relevant to several critical cell functions (e.g., cell proliferation and migration). Furthermore, the majority of these PCN-induced DE genes in HUAECs are not directly regulated by HIF.

To verify the microarray result, qPCR analysis was conducted for a total of nine genes (eight DE and one unchanged gene) (Fig. 4A). All nine genes exhibited changes similar to those found in the microarray analysis ($R^2 = 0.81$; Fig. 4B), indicating that the microarray data accurately predicted the PCN-induced fold change in mRNA. To further verify the microarray results, 10 proteins were examined by

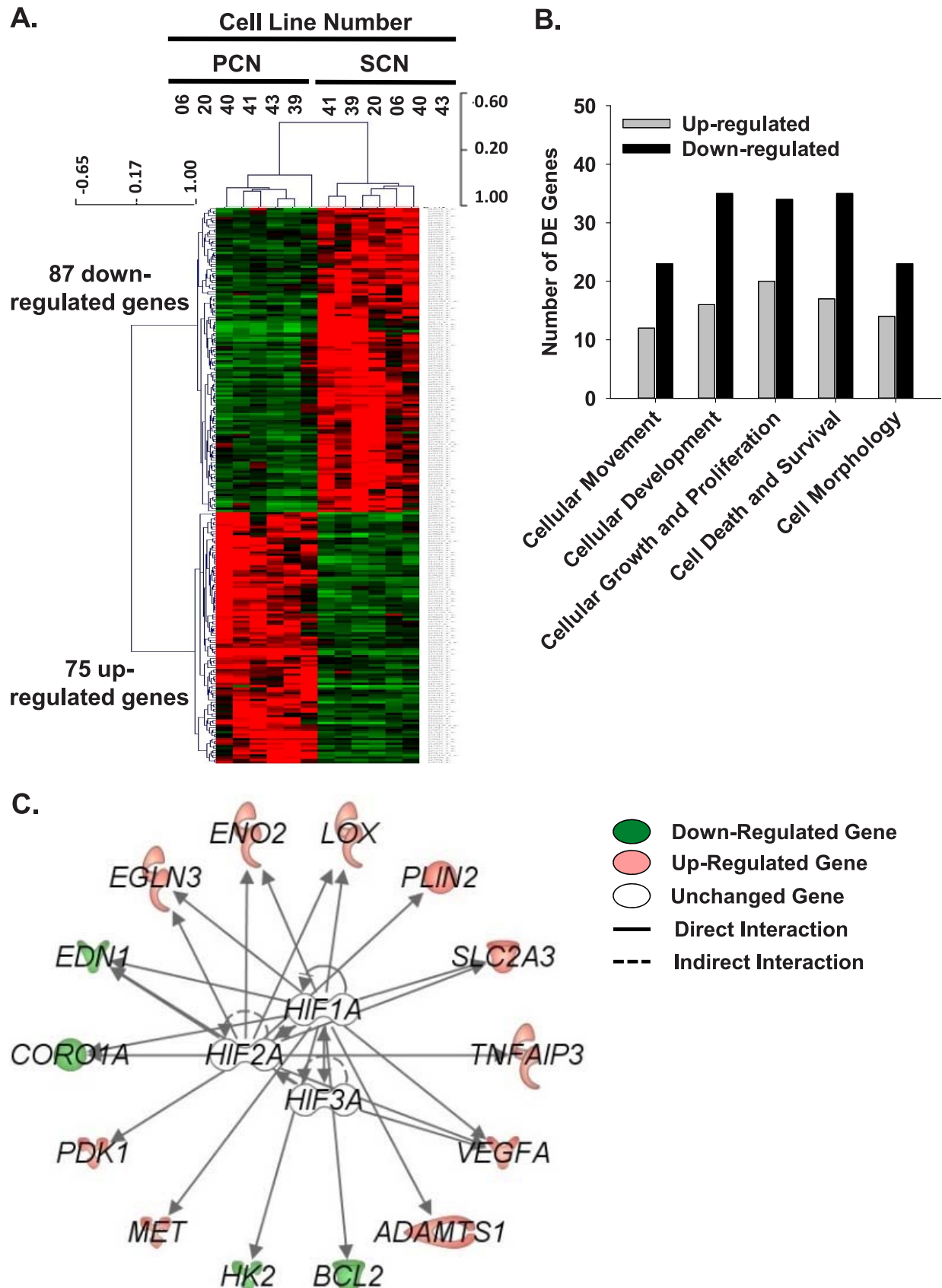


FIG. 3. Microarray analyses of PCN-regulated genes relative to SCN. **A**) Unsupervised two-dimensional hierarchical clustering (Pearson correlation) of the probe sets. **B**) Ingenuity pathway analysis of the cellular functions of PCN-induced DE genes relative to SCN. **C**) Literature mining of DE genes regulated by HIF. *ADAMTS1*: ADAM metalloproteinase with thrombospondin type 1 motif, 1; *BCL2*: B-cell CLL/lymphoma 2; *CORO1A*: coronin, actin binding protein, 1A; *EDN1*: endothelin 1; *EGLN3*: egl nine homolog 3 (*Caenorhabditis elegans*); *ENO2*: enolase 2 (gamma, neuronal); *HK2*: hexokinase 2; *LOX*: lysyl oxidase; *MET*: met proto-oncogene (hepatocyte growth factor receptor); *PDK1*: pyruvate dehydrogenase kinase, isozyme 1; *PLIN2*: perilipin 2; *SLC2A3*: solute carrier family 2 (facilitated glucose transporter), member 3; *TNFAIP3*: tumor necrosis factor, alpha-induced protein 3; *VEGFA*: vascular endothelial growth factor A.

HUMAN ARTERY ENDOTHELIAL CELLS IN CHRONIC LOW O₂

TABLE 1. PCN-induced DE genes with fold changes ≥ 2 in HUAECs.^a

No.	Gene symbol/ probe sets	Gene name	Fold increase
1	<i>CLDN10</i>	Claudin 10	6.6
2	<i>WDR69</i>	WD repeat domain 69	4.1
3	<i>GIPC2</i>	GIPC PDZ domain containing family, member 2	4.0
4	<i>CYB5R2</i>	Cytochrome b5 reductase 2	3.6
5	<i>SSTR1</i>	Somatostatin receptor 1	3.3
6	<i>DPP4</i>	Dipeptidyl-peptidase 4 (CD26, adenosine deaminase complexing protein 2)	3.2
7	<i>CDCP1</i>	CUB domain containing protein 1	3.1
8	<i>IL33</i>	Interleukin 33	3.0
9	<i>AK4</i>	Adenylate kinase 4	2.9
10	<i>CLEC4GP1</i>	C-type lectin domain family 4, member G pseudogene 1	2.7
11	<i>PCDH7</i>	Protocadherin 7	2.6
12	<i>B3GALNT1</i>	Beta-1,3-N-acetylgalactosaminyltransferase 1 (globoside blood group)	2.5
13	<i>GNA14</i>	Guanine nucleotide binding protein (G protein), alpha 14	2.5
14	<i>HSPA12B</i>	Heat shock 70 kD protein 12B	2.5
15	<i>AK3L1</i>	Adenylate kinase 3-like 1	2.4
16	<i>MYRIP</i>	Myosin VIIA and Rab interacting protein	2.4
17	<i>ADAMTS1</i>	ADAM metalloproteinase with thrombospondin type 1 motif, 1	2.3
18	<i>EGLN3</i>	egl nine homolog 3 (<i>C. elegans</i>)	2.3
19	<i>FAM129A</i>	Family with sequence similarity 129, member A	2.3
20	<i>TNFAIP3</i>	Tumor necrosis factor, alpha-induced protein 3	2.3
21	<i>ZNF655</i>	Zinc finger protein 655	2.3
22	<i>CPXM2</i>	Carboxypeptidase X (M14 family), member 2	2.2
23	<i>242057_at</i>	N.A.	2.1
24	<i>ARRDC4</i>	Arrestin domain containing 4	2.1
25	<i>ATP8A2</i>	ATPase, aminophospholipid transporter-like, Class I, type 8A, member 2	2.1
26	<i>PRKAA2</i>	Protein kinase, AMP-activated, alpha 2 catalytic subunit	2.1
27	<i>SEMA4B</i>	Sema domain, immunoglobulin domain (Ig), transmembrane domain (TM) and short cytoplasmic domain, (semaphorin) 4B	2.1
28	<i>ENO2</i>	Enolase 2 (gamma, neuronal)	2.0
29	<i>GRAMD3</i>	GRAM domain containing 3	2.0
30	<i>LOC731884</i>	Similar to programmed cell death 6 interacting protein	2.0
31	<i>PRTFDC1</i>	Phosphoribosyltransferase domain containing 1	2.0
32	<i>SLC38A5</i>	Solute carrier family 38, member 5	2.0
1	<i>FAT3</i>	FAT tumor suppressor homolog 3 (<i>Drosophila</i>)	-4.3
2	<i>CD24</i>	CD24 molecule	-3.3
3	<i>CDH6</i>	Cadherin 6, type 2, K-cadherin (fetal kidney)	-3.1
4	<i>SNAI2</i>	Snail homolog 2 (<i>Drosophila</i>)	-3.1
5	<i>CHRNA1</i>	Cholinergic receptor, nicotinic, alpha 1 (muscle)	-2.8
6	<i>TFEC</i>	Transcription factor EC	-2.8
7	<i>EPHB1</i>	EPH receptor B1	-2.7
8	<i>FLRT3</i>	Fibronectin leucine rich transmembrane protein 3	-2.7
9	<i>FBXL16</i>	F-box and leucine-rich repeat protein 16	-2.6
10	<i>KLRC4</i>	Killer cell lectin-like receptor subfamily C, member 4	-2.6
11	<i>LOC727930</i>	Similar to CG10275-PA	-2.6
12	<i>GDF15</i>	Growth differentiation factor 15	-2.5
13	<i>POPDC3</i>	Popeye domain containing 3	-2.5
14	<i>ANTXR1</i>	Anthrax toxin receptor 1	-2.4
15	<i>BMPRI1B</i>	Bone morphogenetic protein receptor, type IB	-2.4
16	<i>IL11</i>	Interleukin 11	-2.4
17	<i>MLL11</i>	Myeloid/lymphoid or mixed-lineage leukemia (trithorax homolog, <i>Drosophila</i>); translocated to, 11	-2.4
18	<i>FLRT2</i>	Fibronectin leucine rich transmembrane protein 2	-2.3
19	<i>C13orf15</i>	Chromosome 13 open reading frame 15	-2.2
20	<i>PTPRS</i>	Protein tyrosine phosphatase, receptor type, S	-2.2
21	<i>VCAN</i>	Versican	-2.2
22	<i>PBX1</i>	Pre-B-cell leukemia homeobox 1	-2.1
23	<i>PCDH17</i>	Protocadherin 17	-2.1
24	<i>SHC4</i>	SHC (Src homology 2 domain containing) family, member 4	-2.1
25	<i>ZNF117</i>	Zinc finger protein 117	-2.1
26	<i>ZNF365</i>	Zinc finger protein 365	-2.1
27	<i>BEX1</i>	Brain expressed, X-linked 1	-2.0
28	<i>EBF1</i>	Early B-cell factor 1	-2.0
29	<i>ELOVL4</i>	Elongation of very long chain fatty acids (FEN1/Elo2, SUR4/Elo3, yeast)-like 4	-2.0
30	<i>HTRA1</i>	HtrA serine peptidase 1	-2.0
31	<i>NHS</i>	Nance-Horan syndrome (congenital cataracts and dental anomalies)	-2.0
32	<i>NUDT11</i>	Nudix (nucleoside diphosphate linked moiety X)-type motif 11	-2.0
33	<i>SERPINE2</i>	Serpin peptidase inhibitor, clade E (nexin, plasminogen activator inhibitor type 1), member 2	-2.0

^a The fold change was the mean of fold change of probe sets; N.A. = no annotation.

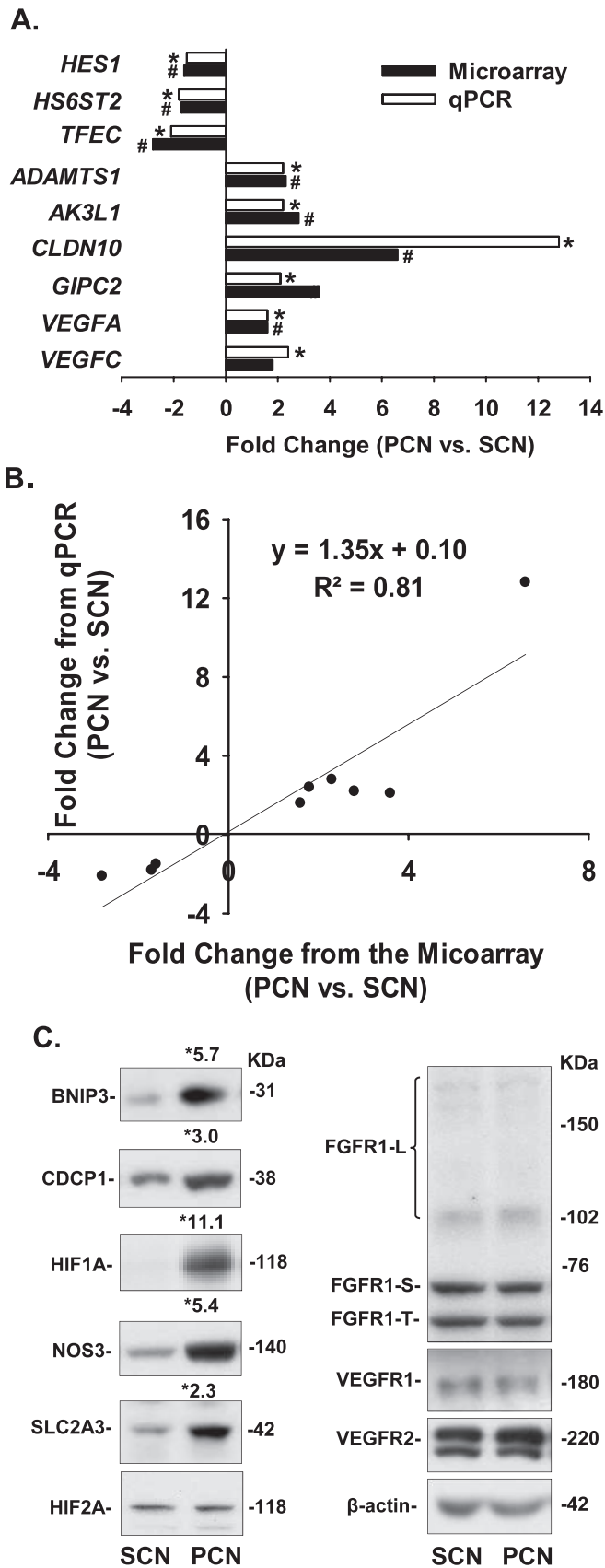


FIG. 4. Quantitative PCR and Western blot analyses. **A, B** Comparison and correlation between qPCR and microarray data. Data are expressed as the mean fold change of SCN. *#Differ from SCN for each analysis ($P < 0.05$, $n = 6$ cell preparations). *ADAMTS1*: ADAM metalloproteinase with thrombospondin type 1 motif, 1; *AK3L1*: adenylate kinase 3-like 1; *CLDN10*: claudin 10; *GIPC2*: GIPC PDZ domain containing family,

Western blot analysis. We observed that 8 out of 10 proteins displayed changes similar to their mRNA counterparts; both the mRNA and protein levels of CDCP1, BNIP3, and SLC2A3 were increased in PCN cells relative to those in SCN cells, and both the mRNA and protein levels of HIF2A, FGFR1, VEGFR1, VEGFR2, and β -actin were similar between PCN and SCN cells. By contrast, PCN elevated the levels of NOS3 and HIF1A protein, but not mRNA compared with those for SCN. These discordances between protein and mRNA levels are believed to be due to posttranscriptional modification of proteins [41] as previously described [10, 11, 42–44].

PCN did increase mRNA levels of VEGFA (Supplemental Table S3) but did not significantly alter either the FGF2, FGFR1, VEGFR1, or VEGFR2 mRNA levels (not shown) or the FGFR1, VEGFR1, and VEGFR2 protein levels (Fig. 2C). Moreover, 91% of the FGFR1 probe sets were present, whereas 91% probe sets for *FGFR2*, 75% of *FGFR3*, and 100% for *FGFR4* were absent, implying that *FGFR1* is the major FGF receptor in HUAECs, a finding that is similar to the situation in HUVECs [21].

DISCUSSION

In this study, we have established HUAECs models in vitro under a physiological O_2 level [6] and provided clear evidence showing that PCN drastically enhances FGF2- and VEGFA-induced cell proliferation and migration and alters the transcriptional profiles in human fetoplacental artery endothelial cells. These PCN-enhanced cellular responses are accompanied by increased expression of HIF1A but without increases in HIF2A and the major FGF and VEGFA receptors. Thus, given that endothelial cells usually live under PCN in vivo, these PCN HUAECs likely represent unique human fetoplacental artery endothelial models that more closely reflect in vivo states.

Recently, the importance of the physiological chronic low O_2 level has begun to be recognized as a key factor to consider in cell culture models [21, 45–48]. For instance, the derivation and expansion of human embryonic stem cells in physiological normoxia ($\sim 5\% O_2$) aid in maintaining cellular pluripotency and suppressing spontaneous cellular differentiation while they enhance the production efficiency of human cardiac stem cells and cell potency for myocardial repair [47]. Similarly, HUVECs cultured and expanded in 3% O_2 exhibit dramatic alterations in their transcriptional profiles and substantial increases in their cellular responses to FGF2 and VEGFA relative to those of HUVECs derived in ambient O_2 [21]. Together with the current observations in HUAECs, these findings clearly indicate that the physiological chronic low O_2 level is indeed critical in the modulation of proliferation and migration of endothelial cells in fetoplacental artery and vein,

member 2; *VEGFA*: vascular endothelial growth factor A; *VEGFC*: vascular endothelial growth factor C. *HES1*: hairy and enhancer of split 1; *HS6ST2*: heparan sulfate 6-O-sulfotransferase 2; *T FEC*: transcription factor EC. **C**) Western blot analysis of PCN-induced DE and unchanged genes. Data normalized to β -actin are expressed as the mean fold change of SCN as indicated. *Differ from SCN ($P < 0.05$, $n = 4$). BNIP3: BCL2/adenovirus E1B 19kDa interacting protein 3; CDCP1: CUB domain containing protein 1; FGFR1-L: fibroblast growth factor receptor 1 (FGFR1)-long form; FGFR1-S, FGFR1-short form; FGFR1-T: FGFR1-truncated form; HIF1A: hypoxia inducible factor 1, α subunit; HIF2A: hypoxia inducible factor 2, α subunit; NOS3: nitric oxide synthase 3, endothelial cell; SLC2A3: solute carrier family 2 (facilitated glucose transporter), member 3; VEGFR1: VEGF receptor 1; VEGFR2: VEGF receptor 2.

especially because even an acute O₂ elevation may dampen cell proliferation and/or migration (Fig. 2, C and D) [21].

A follow-up question we addressed herein is whether these PCN-enhanced cell responses are mediated via increasing the expression of growth factors and their receptors, all of which are considered to be the hallmarks for the hypoxia regulation of endothelial cells [10, 11]. Although PCN enhanced the VEGFA mRNA, PCN did not increase the mRNA and/or protein expression of FGF2, FGFR1, VEGFR1, and VEGFR2 (Fig. 4C). Thus, although increased VEGFA expression may partially contribute to the PCN-enhanced HUAECs responses to VEGFA, the elevated expression of these growth factor receptors in HUAECs is unlikely to have a major effect on these PCN-enhanced cellular responses, and other mechanisms must be involved. One such mechanism could occur via increased activation of these receptors, followed by enhanced activation of protein kinases as occurs in HUVECs [21]. In contrast, altering expression of certain genes that are either stimulatory or inhibitory to these cell responses may lead to these PCN-enhanced angiogenic responses. Examples of these genes may include *ADAMTS1*, a matrix metalloproteinase protein that was up-regulated in PCN (Table 1), and *HES1*, which was down-regulated in PCN (Supplemental Table S3) because *ADAMTS1* promotes the proliferation and migration of HUVEC under hypoxic conditions [49] and *HES1* inhibits the proliferation of human microvascular endothelial cells and human iliac artery endothelial cells [50].

One of the key findings from the current study is that acutely (up to 24 h) increasing the O₂ levels significantly inhibited FGF2- and VEGFA-induced PCN cell migration but not proliferation; in contrast acutely (up to 24 h) decreasing the O₂ levels promoted the FGF2- and VEGF-induced SCN cell proliferation and migration. Although such extreme changes in O₂ may never occur within the placenta in vivo, these findings suggest that the FGF2- and VEGFA-stimulated migration of PCN cells is much more sensitive to O₂ fluctuation than proliferation. More importantly, these observations indicate that an acute decrease in O₂ from a hyperoxic to a more physiological level can benefit endothelial proliferation and migration, two essential steps of neovascularization; however, even an acute increase in O₂ from a physiological to a hyperoxic level could significantly dampen endothelial migration.

Mammalian cells are believed to mainly sense decreases through HIF, in which HIF1A is the major isoform responsible for such sensitivity and for the initiation of subsequent cellular responses [10, 11]. Intriguingly, IPA predicted that 8.8% of the PCN-induced DE genes in HUAECs are directly regulated by HIF1A, HIF2A, and HIF3A (Fig. 1C). These percentages of HIF-regulated DE genes in HUAECs appear to be much lower than the percentage of genes (~30%, 570 out of 1719 DE genes) reported to be directly regulated by HIF1A in human pulmonary artery endothelial cells (HPAECs) [51] that were expanded in ambient O₂ followed by exposure to 1% O₂ for 24 h or overexpressing a constitutively active form of HIF1A. In these 570 HIF1A-regulated genes in HPAECs, only seven genes overlap with those identified in HUAECs (*EDN1*, *EGLN3*, *ENO2*, *LOX*, *SLC2A3*, *TNFAIP3*, and *VEGFA*; Fig. 3C). It is plausible that these differences can be largely attributed to distinctions in cell origins, culture conditions including different O₂ levels (1% vs. 3%), and/or microarray analysis methodologies. However, these findings also suggest that those cells cultured and expanded in ambient O₂ are more sensitive to O₂ regulators. By contrast, HIF1A might be partially transcriptional insensitive because it is maintained at a relatively high level in the PCN HUAECs. Thus, factors other

than HIF must be responsible for the altered expression of these non-HIF-regulated DE genes. In this regard, the participation of two transcription factors, *Myc* and *JUN*, in such regulation has been reported [52, 53]. In addition, the expression of these non-HIF-regulated DE genes could be controlled via epigenetic mechanisms. For example, the DNA methyltransferase 3 alpha (*DNMT3A*), an enzyme that methylates cytosine in the genome causing gene silencing, is upregulated in PCN HUAECs (Supplemental Table S3). Specific histone codes and micro-RNAs may also be involved in such regulation [54, 55]. For example, exposing HUVECs to 1% O₂ for 24 h can induce histone acetylation and methylation in the gene promoter [54].

In conclusion, the current study has clearly demonstrated that similar to HUVECs [21], PCN also programs HUAECs to undergo remarkable changes in cell proliferation and migration in responses to FGF2 and VEGFA and the global gene expression. These data further support the notion that we may have to reevaluate most, if not all, cellular and molecular mechanisms governing endothelial growth and function, which has also been indicated in other types of cells [21, 45–48], using endothelial models cultured and expanded under PCN.

ACKNOWLEDGMENT

We thank Dr. Ronald R. Magness from Department of Obstetrics and Gynecology, University of Wisconsin, Madison, for critically reading and editing this manuscript.

REFERENCES

1. Reynolds LP, Redmer DA. Angiogenesis in the placenta. *Biol Reprod* 2001; 64:1033–1040.
2. Benirschke K, Kaufmann P, Baergen BN. Anatomy and pathology of the umbilical cord. In: Benirschke K, Kaufmann P, Baergen BN (eds.), *Pathology of the Human Placenta*. 5th ed. New York: Springer; 2006:380–451.
3. Magness RR, Zheng J. Circulatory changes during gestation. In: Gluckman PD, Heymann MA (eds.), *Pediatric and Perinatal Medicine: The Scientific Basis*. London: Edward Arnold Publishers; 1996:762–772.
4. Osol G, Mandala M. Maternal uterine vascular remodeling during pregnancy. *Physiology (Bethesda)* 2009; 24:58–71.
5. Wang K, Zheng J. Signaling regulation of fetoplacental angiogenesis. *J Endo* 2012; 212:243–255.
6. Rodesch F, Simon P, Donner C, Jauniaux E. Oxygen measurements in endometrial and trophoblastic tissues during early pregnancy. *Obstet Gynecol* 1992; 80:283–285.
7. Wareing M, Greenwood SL, Baker PN. Reactivity of human placental chorionic plate vessels is modified by level of oxygenation: differences between arteries and veins. *Placenta* 2006; 27:42–48.
8. Zamudio S. High-altitude hypoxia and preeclampsia. *Front Biosci* 2007; 12:2967–2977.
9. Mayhew TM. Changes in fetal capillaries during preplacental hypoxia: growth, shape remodelling and villous capillarization in placentae from high-altitude pregnancies. *Placenta* 2003; 24:191–198.
10. Pugh CW, Ratcliffe PJ. Regulation of angiogenesis by hypoxia: role of the HIF system. *Nat Med* 2003; 9:677–684.
11. Semenza GL. Hypoxia-inducible factors in physiology and medicine. *Cell* 2012; 148:399–408.
12. Burton GJ, Reshetnikova OS, Milovanov AP, Teleshova OV. Stereological evaluation of vascular adaptations in human placental villi to differing forms of hypoxic stress. *Placenta* 1996; 17:49–55.
13. Savransky V, Nanayakkara A, Li J, Bevans S, Smith PL, Rodriguez A, Polotsky VY. Chronic intermittent hypoxia induces atherosclerosis. *Am J Respir Crit Care Med* 2007; 175:1290–1297.
14. Ferrara N, Gerber HP, LeCouter J. The biology of VEGF and its receptors. *Nat Med* 2003; 9:669–676.
15. Podar K, Anderson KC. The pathophysiologic role of VEGF in hematologic malignancies: therapeutic implications. *Blood* 2005; 105:1383–1395.
16. Turner N, Grose R. Fibroblast growth factor signaling: from development to cancer. *Nat Rev Cancer* 2010; 10:116–129.
17. Humar R, Kiefer FN, Berns H, Resink TJ, Battagay EJ. Hypoxia enhances

- vascular cell proliferation and angiogenesis in vitro via rapamycin (mTOR)-dependent signaling. *FASEB J* 2002; 16:771–780.
18. Meininger CJ, Schelling ME, Granger HJ. Adenosine and hypoxia stimulate proliferation and migration of endothelial cells. *Am J Physiol* 1988; 255:H554–H562.
 19. Phillips PG, Birnby LM, Narendran A. Hypoxia induces capillary network formation in cultured bovine pulmonary microvessel endothelial cells. *Am J Physiol* 1995; 268:L789–L800.
 20. Wang K, Jiang YZ, Chen DB, Zheng J. Hypoxia enhances FGF2- and VEGFA-stimulated human placental artery endothelial cell proliferation: roles of MEK1/2/ERK1/2 and PI3K/AKT pathways. *Placenta* 2009; 30: 1045–1051.
 21. Jiang YZ, Wang K, Li Y, Dai CF, Wang P, Kendzierski C, Chen DB, Zheng J. Transcriptional and functional adaptations of endothelial cells to physiological chronic low oxygen. *Biol Reprod* 2013; 88:114.
 22. Chi JT, Chang HY, Haraldsen G, Jahnsen FL, Troyanskaya OG, Chang DS, Wang Z, Rockson SG, van de Rijn M, Botstein D, Brown PO. Endothelial cell diversity revealed by global expression profiling. *Proc Natl Acad Sci U S A* 2003; 100:10623–10628.
 23. Aitseaomo J, Portbury AL, Schisler JC, Patterson C. Brothers and sisters: molecular insights into arterial-venous heterogeneity. *Circ Res* 2008; 103: 929–939.
 24. Rocha SF, Adams RH. Molecular differentiation and specialization of vascular beds. *Angiogenesis* 2009; 12:139–147.
 25. Lang I, Pabst MA, Hiden U, Blaschitz A, Dohr G, Hahn T, Desoye G. Heterogeneity of microvascular endothelial cells isolated from human term placenta and macrovascular umbilical vein endothelial cells. *Eur J Cell Biol* 2003; 82:163–173.
 26. Min J, Jin YM, Moon JS, Sung MS, Jo SA, Jo I. Hypoxia-induced endothelial NO synthase gene transcriptional activation is mediated through the tax-responsive element in endothelial cells. *Hypertension* 2006; 47:1189–1196.
 27. Olszewska-Pazdrak B, Hein TW, Olszewska P, Carney DH. Chronic hypoxia attenuates VEGF signaling and angiogenic responses by downregulation of KDR in human endothelial cells. *Am J Physiol Cell Physiol* 2009; 296:C1162–C1170.
 28. Matsuo K, Malinow AM, Harman CR, Baschat AA. Decreased placental oxygenation capacity in pre-eclampsia: clinical application of a novel index of placental function performed at the time of delivery. *J Perinat Med* 2009; 37:657–661.
 29. Jobe SO, Ramadoss J, Koch JM, Jiang YZ, Zheng J, Magness RR. Estradiol-17 β and its cytochrome P450- and catechol-O-methyltransferase-derived metabolites stimulate proliferation in uterine artery endothelial cells: role of estrogen receptor-alpha versus estrogen receptor-beta. *Hypertension* 2010; 55:1005–1011.
 30. Dai DF, Jiang YZ, Li Y, Wang K, Liu PS, Patankar MS, Zheng J. Expression and roles of the Slit/Robo in human ovarian cancer. *Histochem Cell Biol* 2011; 135:475–485.
 31. Hill DJ, Tevaarwerk GJ, Arany E, Kilkenny D, Gregory M, Langford KS, Miell J. Fibroblast growth factor-2 (FGF-2) is present in maternal and cord serum, and in the mother is associated with a binding protein immunologically related to the FGF receptor-1. *J Clin Endocrinol Metab* 1995; 80:1822–1831.
 32. Baker PN, Krasnow J, Roberts JM, Yeo KT. Elevated serum levels of vascular endothelial growth factor in patients with preeclampsia. *Obstet Gynecol* 1995; 86:815–821.
 33. Galazios G, Papazoglou D, Giagloglou K, Vassaras G, Koutlaki N, Maltezos E. Umbilical cord serum vascular endothelial growth factor (VEGF) levels in normal pregnancies and in pregnancies complicated by preterm delivery or pre-eclampsia. *Int J Gynaecol Obstet* 2004; 85:6–11.
 34. Wallner W, Sengenberger R, Strick R, Strissel PL, Meurer B, Beckmann MW, Schlembach D. Angiogenic growth factors in maternal and fetal serum in pregnancies complicated by intrauterine growth restriction. *Clin Sci (Lond)* 2007; 112:51–57.
 35. Jelkmann W. Pitfalls in the measurement of circulating vascular endothelial growth factor. *Clin Chem* 2001; 47:617–623.
 36. Chung JY, Song Y, Wang Y, Magness RR, Zheng J. Differential expression of vascular endothelial growth factor (VEGF), endocrine gland derived-VEGF, and VEGF receptors in human placentas from normal and preeclamptic pregnancies. *J Clin Endocrinol Metab* 2004; 89:2484–2490.
 37. Newton MA, Kendzierski CM. Parametric empirical Bayes methods for microarrays. In: Parmigiani G, Garrett ES, Irizarry R, Zeger SL (eds.), *The Analysis of Gene Expression Data: Methods and Software*. New York: Springer Verlag; 2003:254–271.
 38. Saeed AI, Bhagabati NK, Braisted JC, Liang W, Sharov V, Howe EA, Li J, Thiagarajan M, White JA, Quackenbush J. TM4 microarray software suite. *Methods Enzymol* 2006; 411:134–193.
 39. Pfaffl MW, Tichopad A, Prgomet C, Neuvians TP. Determination of stable housekeeping genes, differentially regulated target genes and sample integrity: BestKeeper–Excel-based tool using pair-wise correlations. *Biotechnol Lett* 2004; 26:509–515.
 40. Pfaffl MW, Horgan GW, Dempfle L. Relative expression software tool (REST) for group-wise comparison and statistical analysis of relative expression results in real-time PCR. *Nucleic Acids Res* 2002; 30:e36.
 41. de Sousa Abreu R, Penalva LO, Marcotte EM, Vogel C. Global signatures of protein and mRNA expression levels. *Mol Biosyst* 2009; 5:1512–1526.
 42. Rajakumar A, Conrad KP. Expression, ontogeny, and regulation of hypoxia-inducible transcription factors in the human placenta. *Biol Reprod* 2000; 63:559–569.
 43. Rajakumar A, Whitelock KA, Weissfeld LA, Daftary AR, Markovic N, Conrad KP. Selective overexpression of the hypoxia-inducible transcription factor, HIF-2 α , in placentas from women with preeclampsia. *Biol Reprod* 2001; 64:499–506.
 44. Rajakumar A, Whitelock KA, Weissfeld LA, Daftary AR, Markovic N, Conrad KP. Selective overexpression of the hypoxia-inducible transcription factors in placentas from women with preeclampsia [Erratum]. *Biol Reprod* 2001; 64:1019–1020.
 45. Atkuri KR, Herzenberg LA, Herzenberg LA. Culturing at atmospheric oxygen levels impacts lymphocyte function. *Proc Natl Acad Sci U S A* 2005; 102:3756–3759.
 46. Atkuri KR, Herzenberg LA, Niemi AK, Cowan T, Herzenberg LA. Importance of culturing primary lymphocytes at physiological oxygen levels. *Proc Natl Acad Sci U S A* 2007; 104:4547–4552.
 47. Lengner CJ, Gimelbrant AA, Erwin JA, Cheng AW, Guenther MG, Welstead GG, Alagappan R, Frampton GM, Xu P, Muffat J, Santagata S, Powers D, et al. Derivation of pre-X inactivation human embryonic stem cells under physiological oxygen concentrations. *Cell* 2010; 141:872–883.
 48. Li TS, Cheng K, Malliaras K, Matsushita N, Sun B, Marbán L, Zhang Y, Marbán E. Expansion of human cardiac stem cells in physiological oxygen improves cell production efficiency and potency for myocardial repair. *Cardiovas Res* 2011; 89:157–165.
 49. Hatipoglu OF, Hirohata S, Cilek MZ, Ogawa H, Miyoshi T, Obika M, Demircan K, Shinohata R, Kusachi S, Ninomiya Y. ADAMTS1 is a unique hypoxic early response gene expressed by endothelial cells. *J Biol Chem* 2009; 284:16325–16333.
 50. Liu ZJ, Xiao M, Balint K, Soma A, Pinnix CC, Capobianco AJ, Velazquez OC, Herlyn M. Inhibition of endothelial cell proliferation by Notch1 signaling is mediated by repressing MAPK and PI3K/Akt pathways and requires MAML1. *FASEB J* 2006; 20:1009–1011.
 51. Manalo DJ, Rowan A, Lavoie T, Natarajan L, Kelly BD, Ye SQ, Garcia JG, Semenza GL. Transcriptional regulation of vascular endothelial cell responses to hypoxia by HIF-1. *Blood* 2005; 105:659–669.
 52. Webb JD, Coleman ML, Pugh CW. Hypoxia, hypoxia-inducible factors (HIF), HIF hydroxylases and oxygen sensing. *Cell Mol Life Sci* 2009; 66: 3539–3554.
 53. Mense SM, Sengupta A, Zhou M, Lan C, Bentsman G, Volsky DJ, Zhang L. Gene expression profiling reveals the profound upregulation of hypoxia-responsive genes in primary human astrocytes. *Physiol Genomics* 2006; 25:435–449.
 54. Fish JE, Yan MS, Matouk CC, St Bernard R, Ho JJ, Gavryushova A, Srivastava D, Marsden PA. Hypoxic repression of endothelial nitric-oxide synthase transcription is coupled with eviction of promoter histones. *J Biol Chem* 2010; 285:810–826.
 55. Crosby ME, Devlin CM, Glazer PM, Calin GA, Ivan M. Emerging roles of microRNAs in the molecular responses to hypoxia. *Curr Pharm Des* 2009; 15:3861–3866.